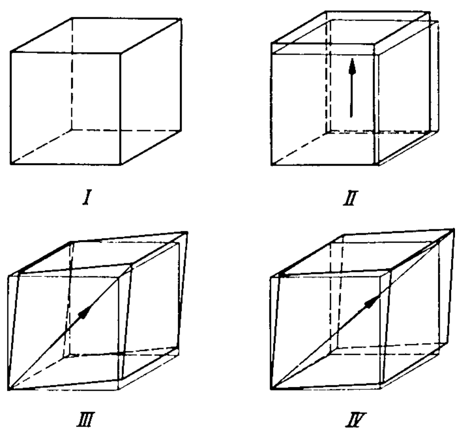

Fig. 1A-10-001. $BaTiO_3$. Pseudocubic cells of the phases I, II, III and IV [66Car]. The arrows show the direction of P_s. The thin lines show the original cubic cell and the bold lines show the pseudocubic cell.

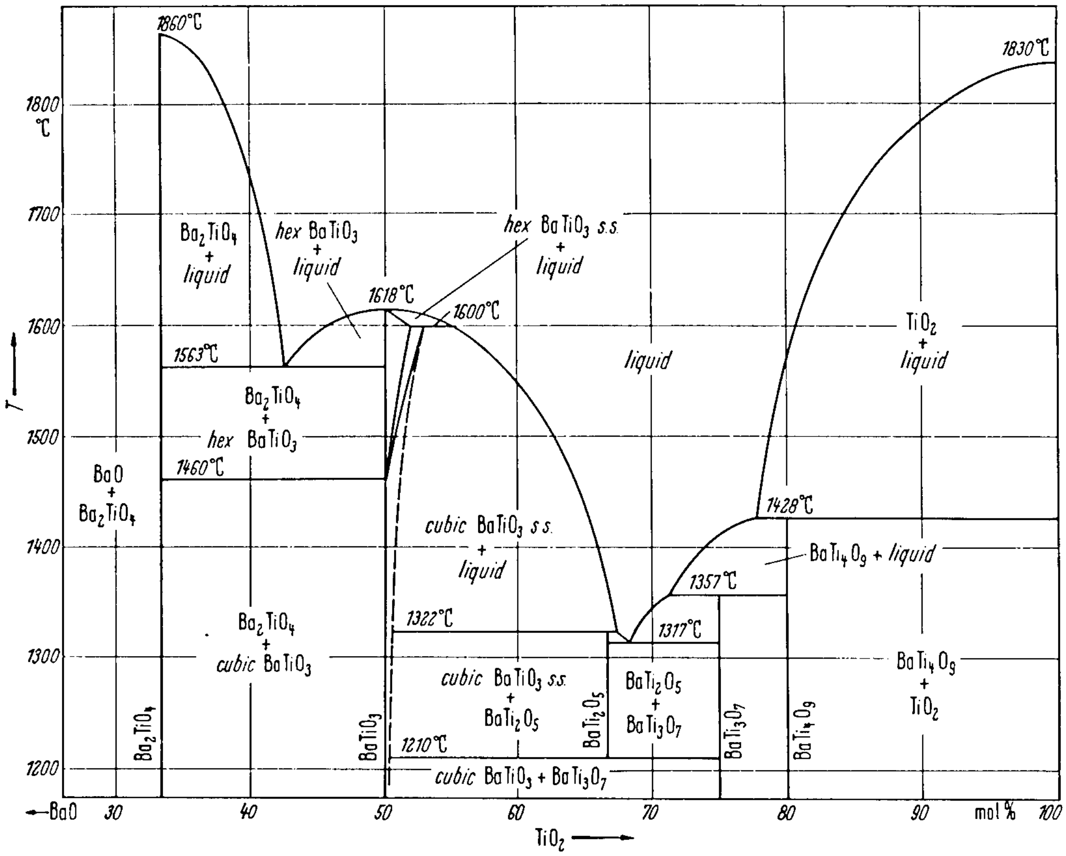

Fig. 1A-10-002. $BaTiO_3$. Equilibrium phase diagram of BaO–TiO_2 system [55Ras].

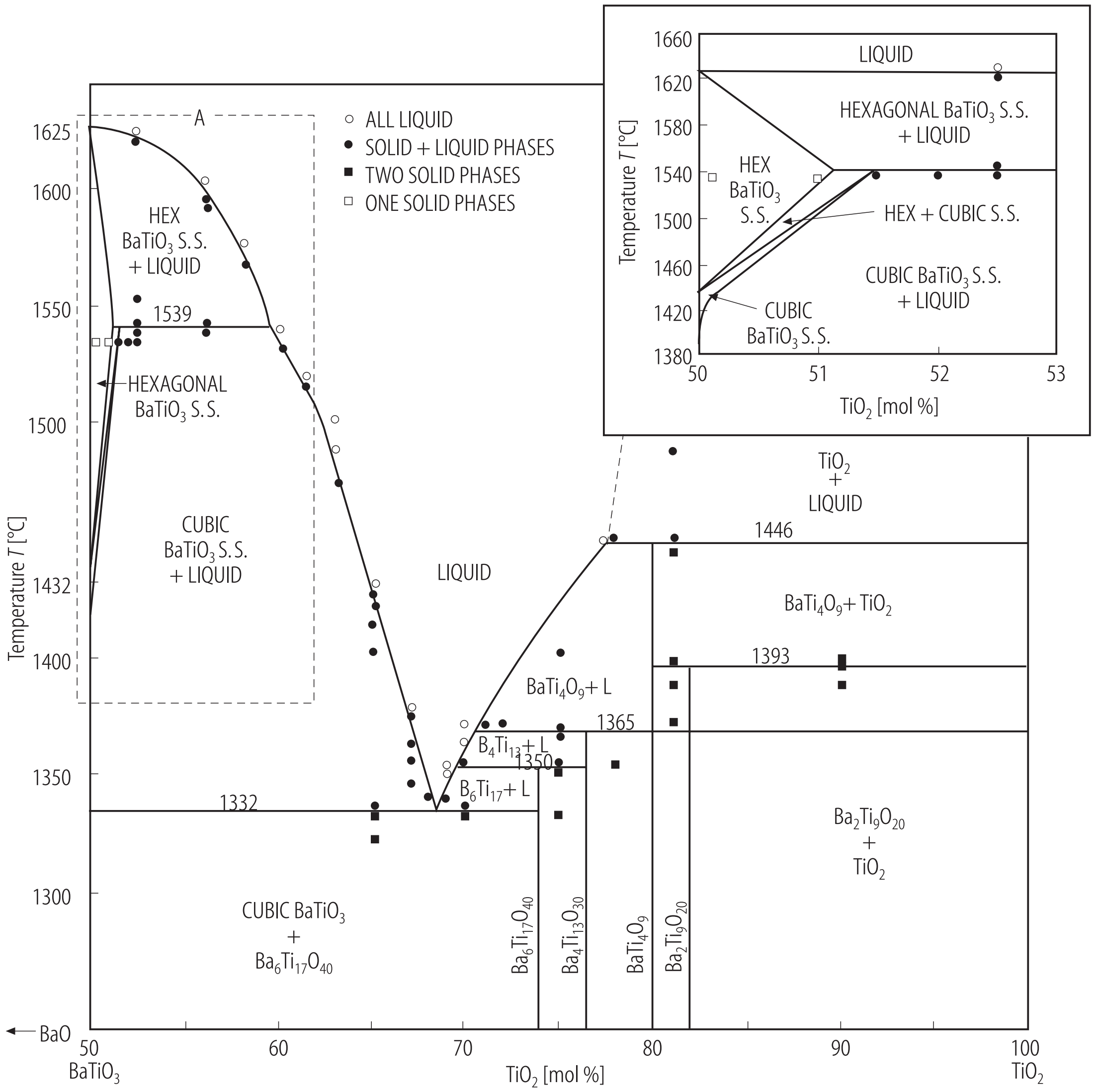

Fig. 1A-10-003. $BaTiO_3$. Equilibrium phase diagram of $BaTiO_3$–TiO_2 system [91Kir]. Composition is given in terms of the components BaO and TiO_2.

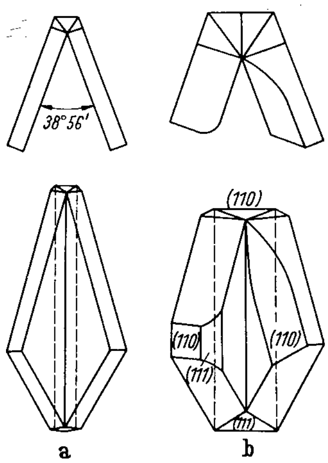

Fig. 1A-10-004. $BaTiO_3$. Small-angle butterfly twin [59DeV]. **(a)** Plane and perspective views of an ideal crystal; all crystal faces are (100) with the exception of (110) spine terminations; composition plane is (111). **(b)** Plane and perspective views of twinned crystals with common growth deviations: (110) and (111) terminations; (110) and approximately (110) and (111) faces.

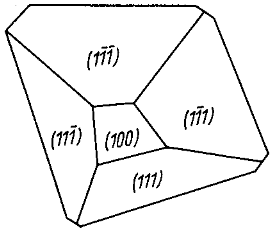

Fig. 1A-10-005. $BaTiO_3$. Form of crystal grown from TiO_2-rich melt [65Sas].

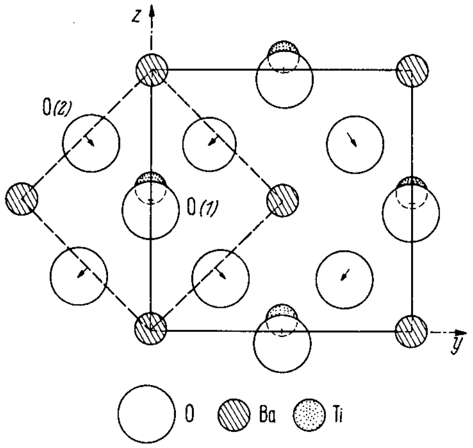

Fig. 1A-10-006. $BaTiO_3$. Projection of the structure of phase III on (100) [57Shi]. The arrows show shifts of ions from the high-symmetry positions occupied in phase I.

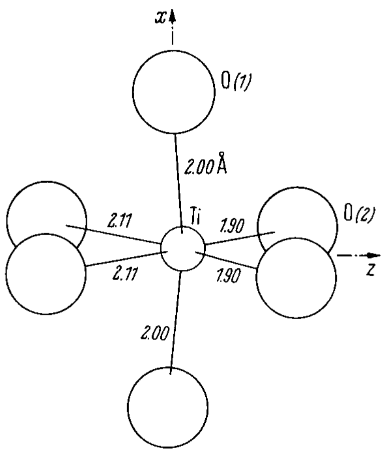

Fig. 1A-10-007. $BaTiO_3$. Environment of Ti in phase III with interatomic distances [57Shi].

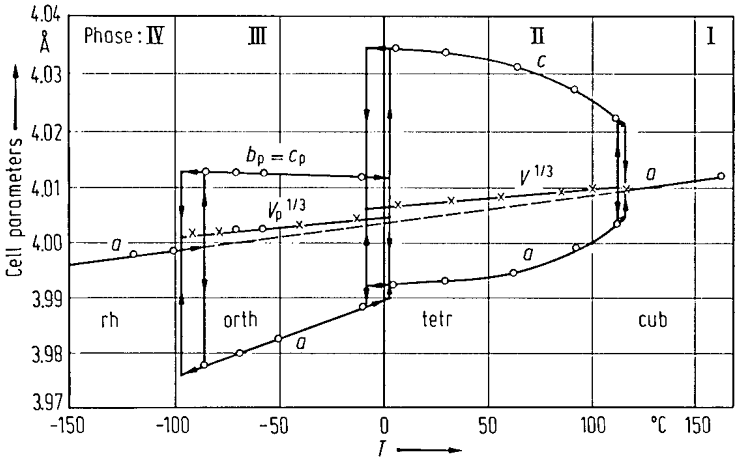

Fig. 1A-10-008. $BaTiO_3$. Cell parameters vs. *T* [49Kay]. *V*: unit cell volume. b_p, c_p, V_p: cell parameters of pseudocubic unit cell (see Fig. 1A-10-001). See also [81She].

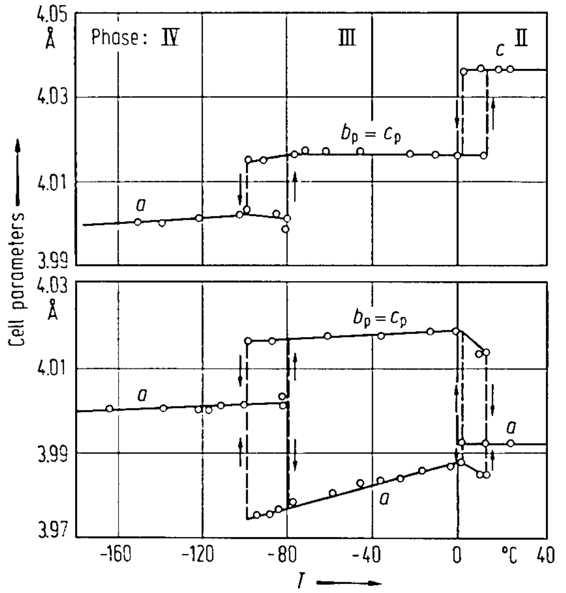

Fig. 1A-10-009. $BaTiO_3$. Cell parameters vs. *T* [49Rho]. Symbols are the same as in Fig. 1A-10-008.

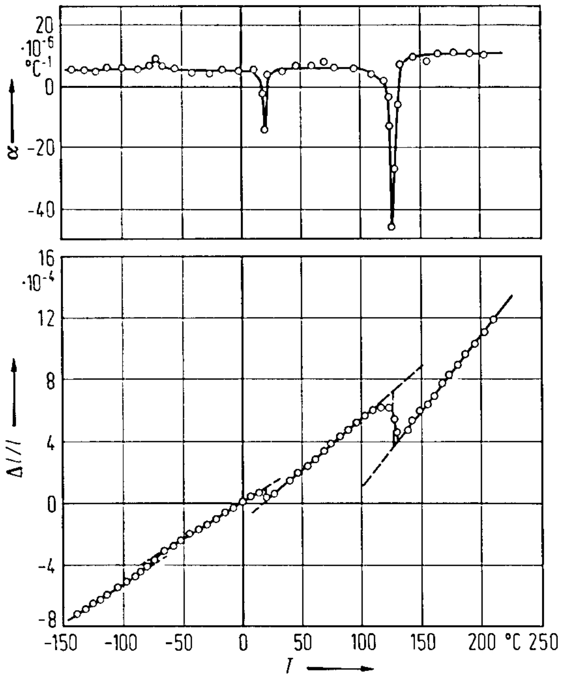

Fig. 1A-10-010. $BaTiO_3$ (ceramics). Δ*l*/*l* and α vs. *T* [52Shi]. Δ*l*/*l*: linear thermal expansion. α: linear thermal expansion coefficient.

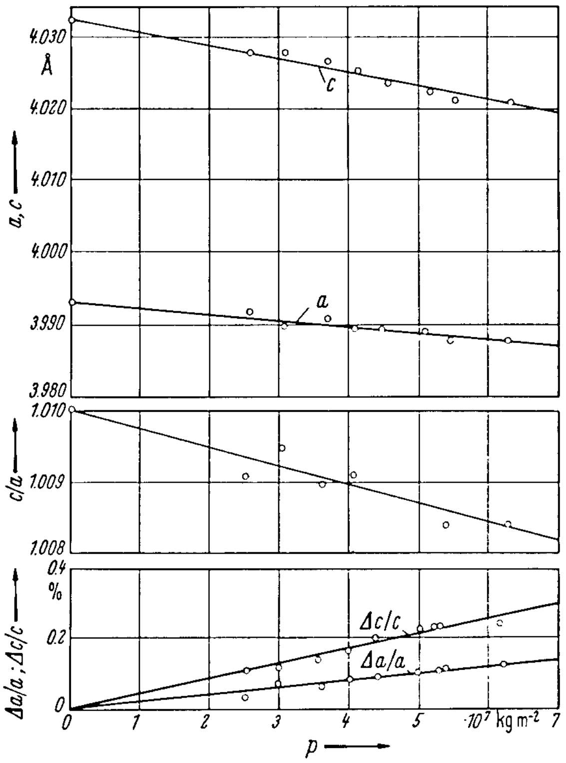

Fig. 1A-10-011. $BaTiO_3$. *a*, *c*, *c/a*, Δ*a/a* and Δ*c/c* vs. *p* in phase II [62Kab]. *p*: hydrostatic pressure.

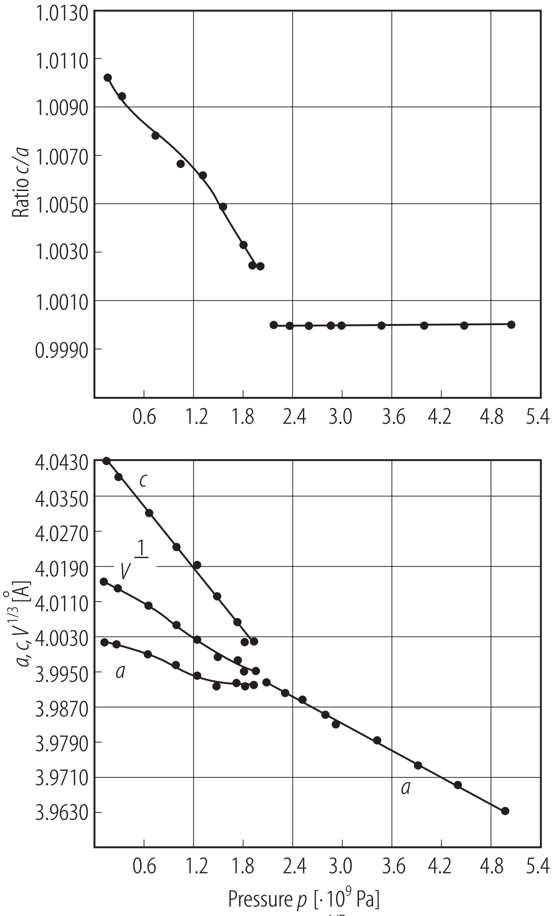

Fig. 1A-10-012. $BaTiO_3$. *a*, *c*, $V^{1/3}$, and *c/a* vs. *p* at 22 °C [86Mal]. *p*: hydrostatic pressure.

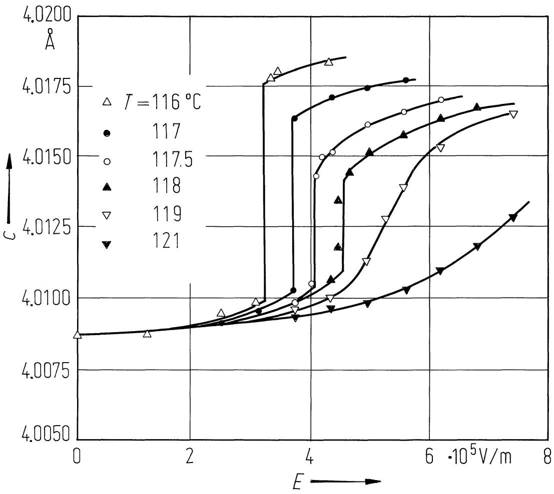

Fig. 1A-10-013. $BaTiO_3$. *c* vs. *E* [85McW]. Parameter: *T*.

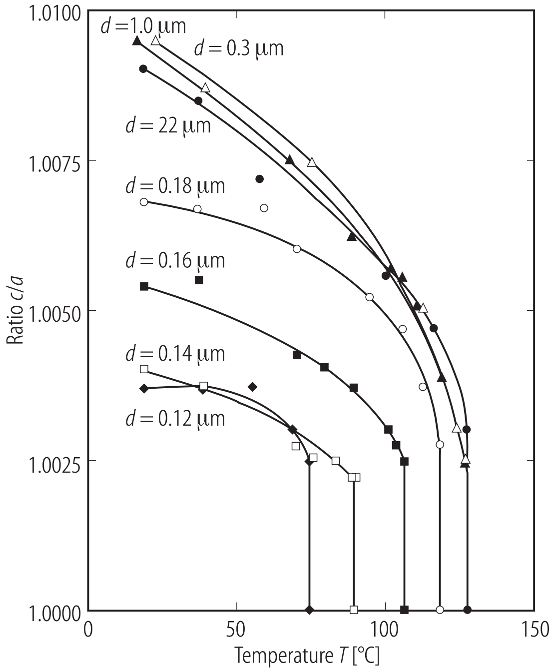

Fig. 1A-10-014. $BaTiO_3$ (ceramics). *c/a* vs. *T* [89Uch]. Parameter: *d*, particle size.

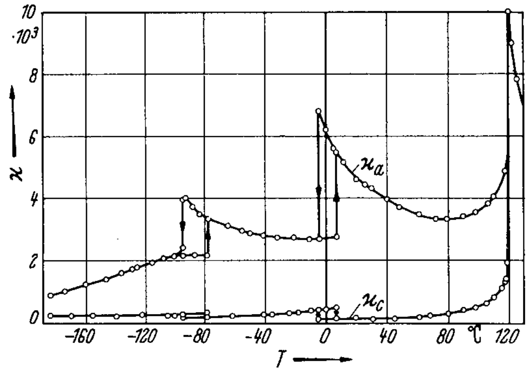

Fig. 1A-10-015. BaTiO$_3$. κ_a, κ_c vs. T [49Mer].

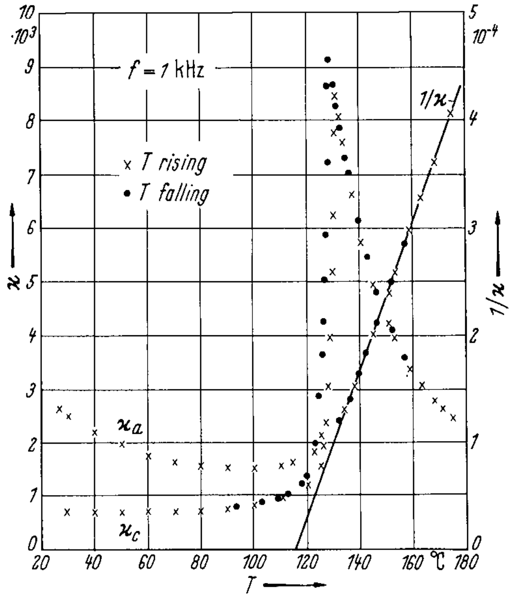

Fig. 1A-10-016. $BaTiO_3$. κ_a, κ_c, κ^{-1} vs. T [65Joh1]. The crystal was grown by pulling method.

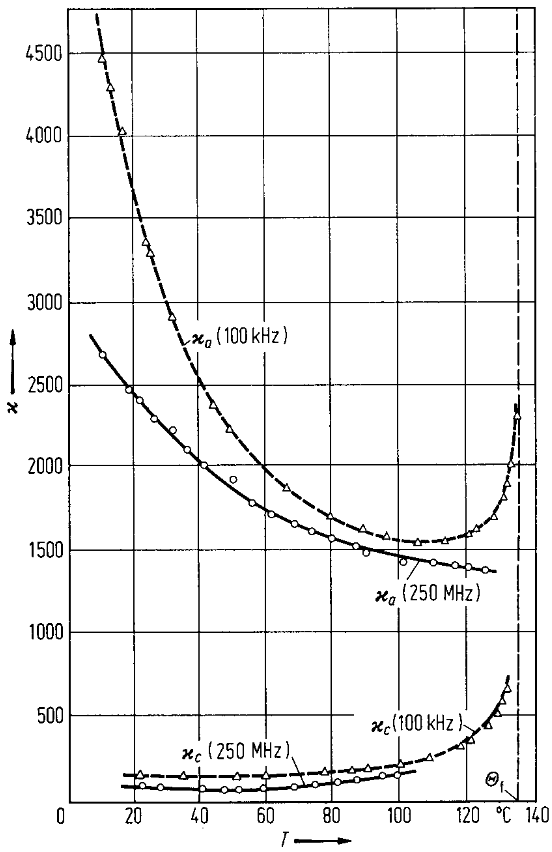

Fig. 1A-10-017. $BaTiO_3$. κ_a, κ_c vs. T in phase II [68Wem]. The crystal was grown by top-seeded solution method. Θ_f = 136(2) °C. Θ_{III-II} = 6(1) °C.

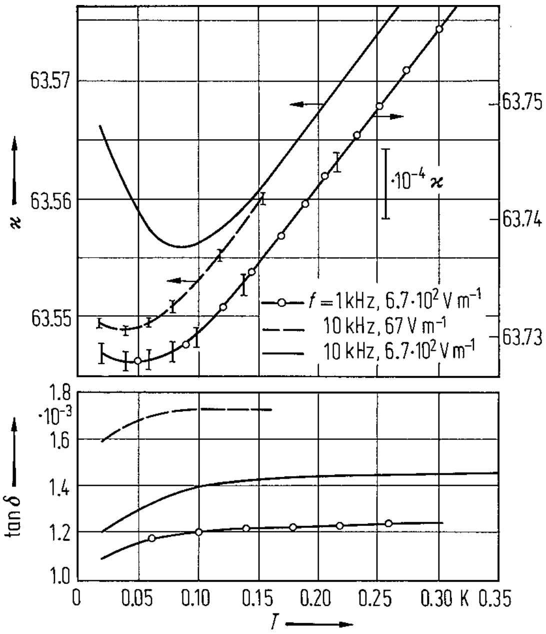

Fig. 1A-10-018. $BaTiO_3$. *κ*, tan *δ* vs. *T* at low temperatures [76Hol]. Parameter: *f*.

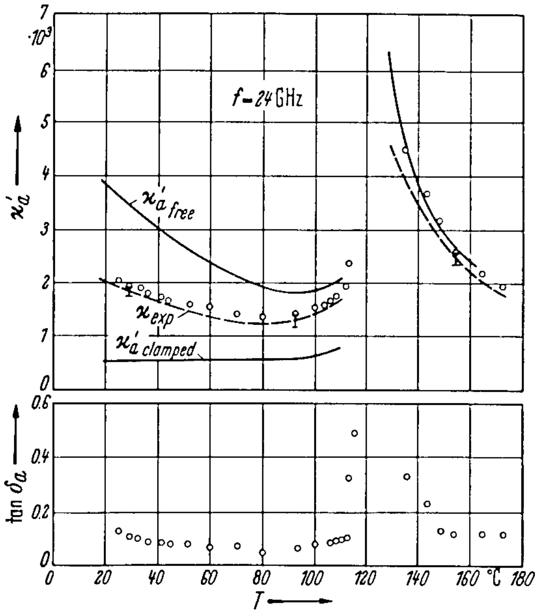

Fig. 1A-10-019. $BaTiO_3$. κ_a', $\tan\delta_a$ vs. T [58Ben]. f = 24 GHz. Circles: 0.0300 cm sample. Dashed lines: average of five samples. Solid lines: Devonshire theory. Vertical bars: spread in value for five samples.

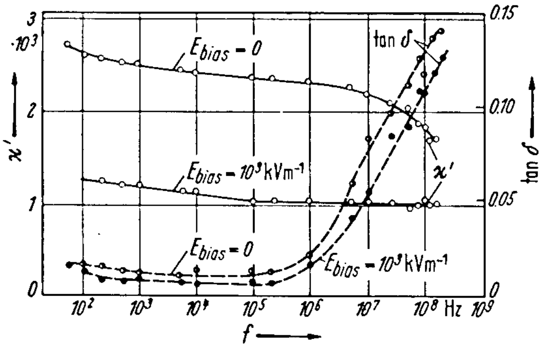

Fig. 1A-10-020. $BaTiO_3$ (multidomain single crystal). κ', $\tan\delta$ vs. f [64Pop]. Parameter: E_{bias}.

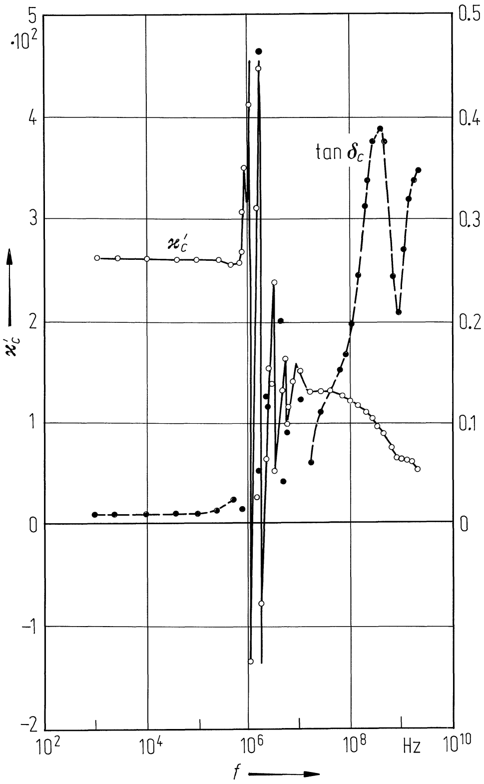

Fig. 1A-10-021. $BaTiO_3$. κ_c', $\tan\delta_c$ vs. f [85Tur]. T =25 °C. $\Theta_{II\text{–}I}$ = 134 °C. Crystal was grown by Linz method.

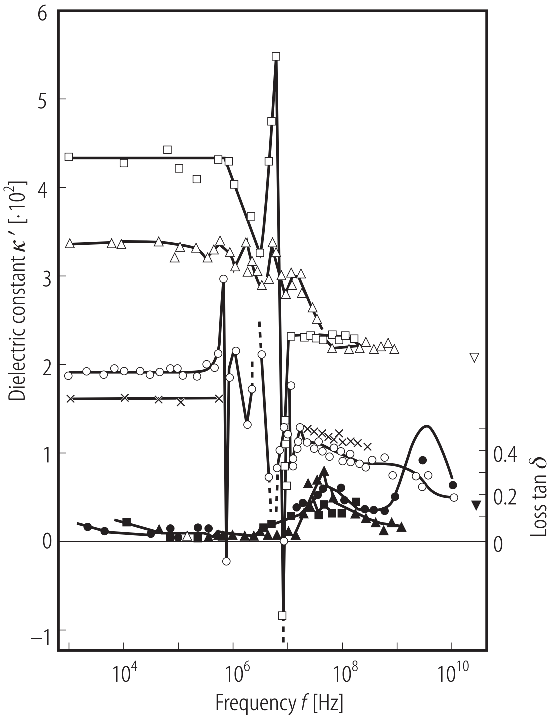

Fig. 1A-10-022. $BaTiO_3$. κ', tan δ vs. *f* [79Tur]. *T* = 25 °C. Open symbols: κ'. Full symbols: tan δ. Squares, downside triangles: single domain crystals along [100] (downside triangles: data from [58Ben]). Upside triangles: 180° polydomain crystals along [100]. Circles: single domain crystals along [001]. Cross: $\kappa'_{[001]}$ of one polydomain crystal.

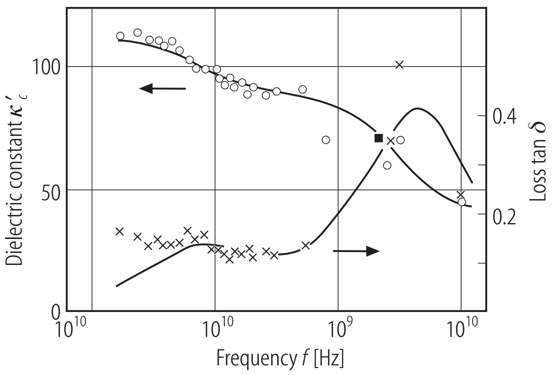

Fig. 1A-10-023. $BaTiO_3$. κ_c', $\tan \delta_c$ vs. f [78Tur]. T = 25 °C. Solid lines are fits to the two Debye dispersion formulae.

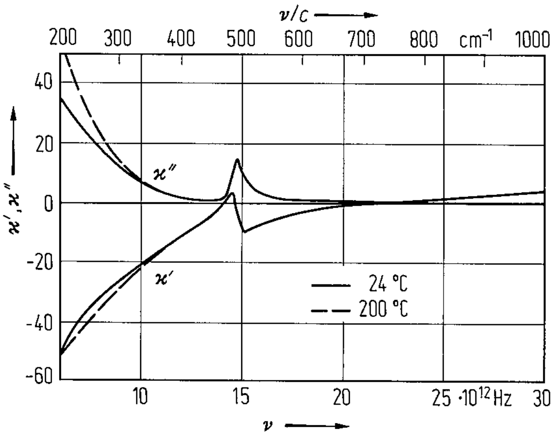

Fig. 1A-10-024. $BaTiO_3$. *κ*' , *κ*'' vs. *ν* [64Bal]. Parameter: *T*.

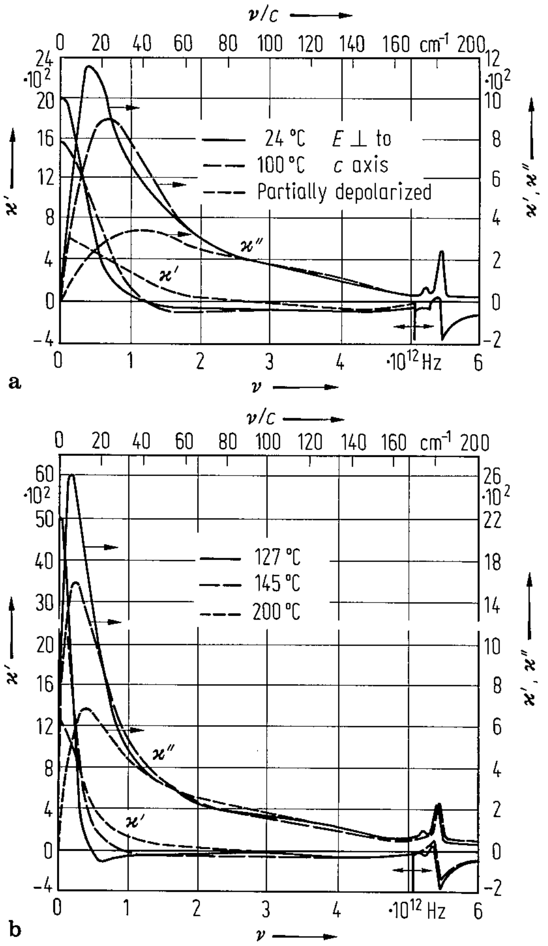

Fig. 1A-10-025. $BaTiO_3$. κ', κ'' vs. ν [64Bal]. Parameter: T. Note change of scale for κ' and κ''.

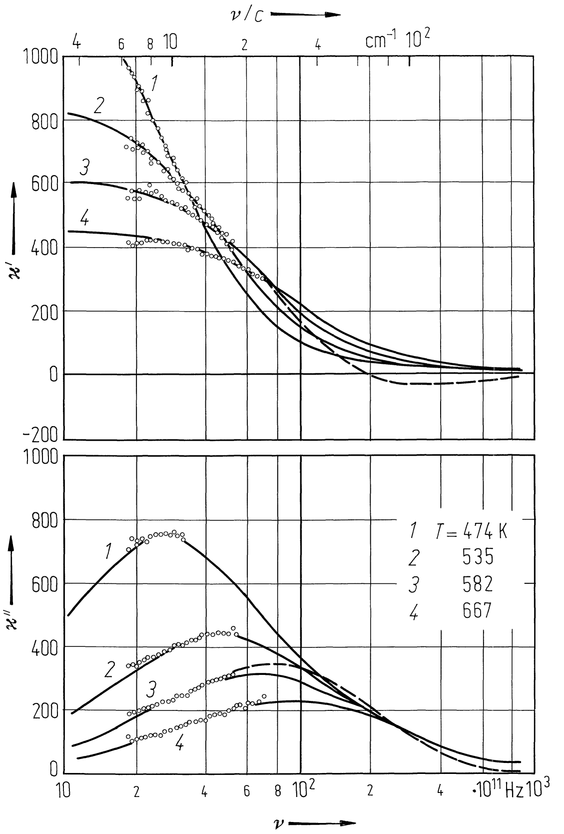

Fig. 1A-10-026. $BaTiO_3$. κ', κ" vs. ν [86Vol]. Parameter: *T*. Full and broken curves are the results of least square fitting for the relaxator model, $\kappa = \kappa_\infty + \Delta\kappa / (1 + i2\pi f \tau)$, and the resonance model $\kappa = \kappa_\infty + \Delta\kappa f^2 / (f^2 - f_0^2 + i\gamma f)$, respectively.

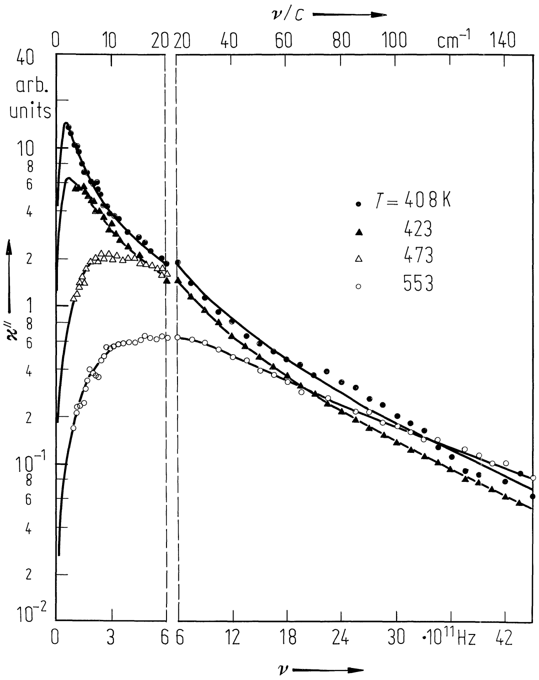

Fig. 1A-10-027. $BaTiO_3$. κ'' vs. ν [82Vog]. Parameter: *T*. κ'' is obtained from hyper-Raman spectrum. Full curves: the fits of the data to the classical oscillator model.

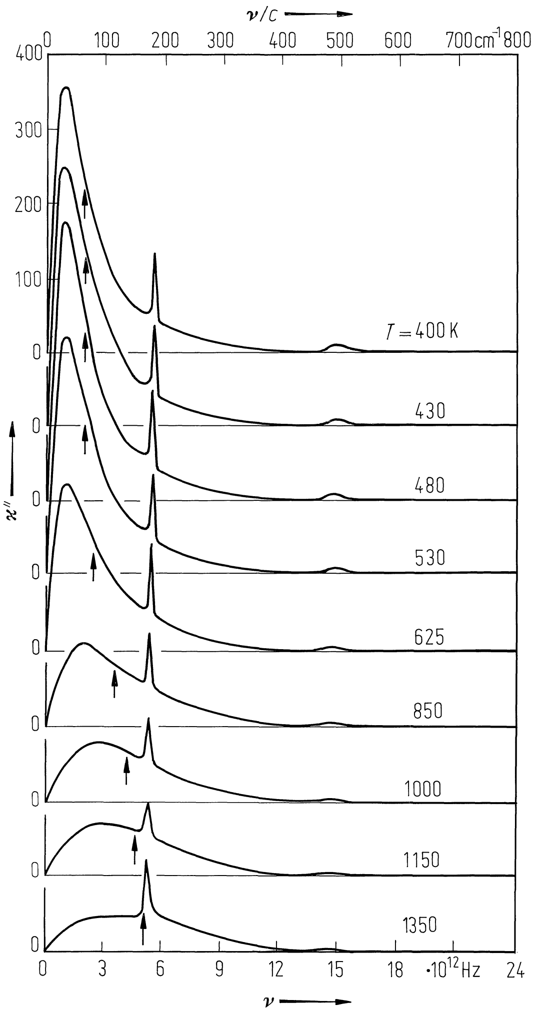

Fig. 1A-10-028. $BaTiO_3$. κ'' vs. ν [80Lus]. Parameter: *T*. Curves were obtained from reflectivity data using Kramers-Kronig relation. The arrows indicate the soft mode frequency obtained from the fit.

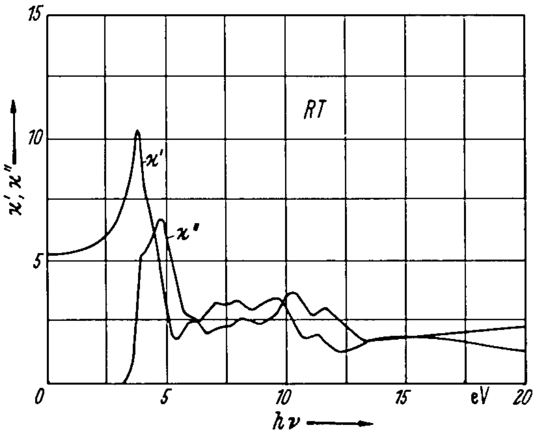

Fig. 1A-10-029. BaTiO$_3$. κ', κ'' vs. $h\nu$ [65Car].

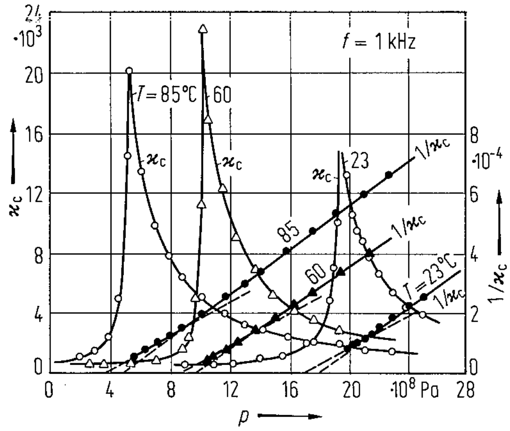

Fig. 1A-10-030. $BaTiO_3$. κ_c, κ_c^{-1} vs. p [66Sam]. Parameter: T.

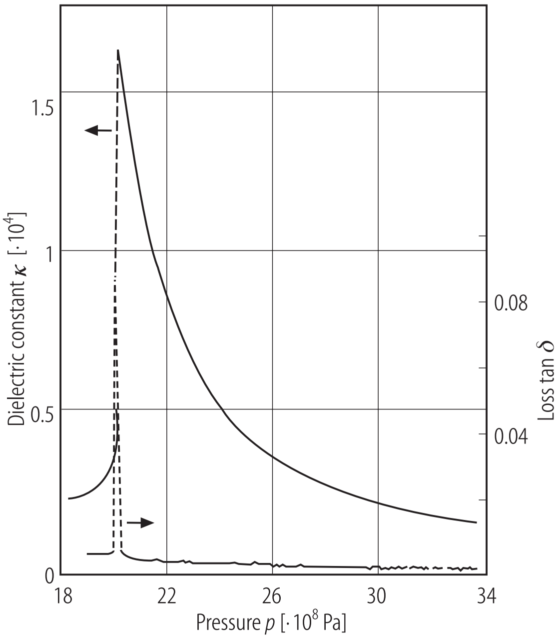

Fig. 1A-10-031. $BaTiO_3$. κ, $\tan\delta$ vs. p [89Dec]. f = 10 kHz. T = 24 °C.

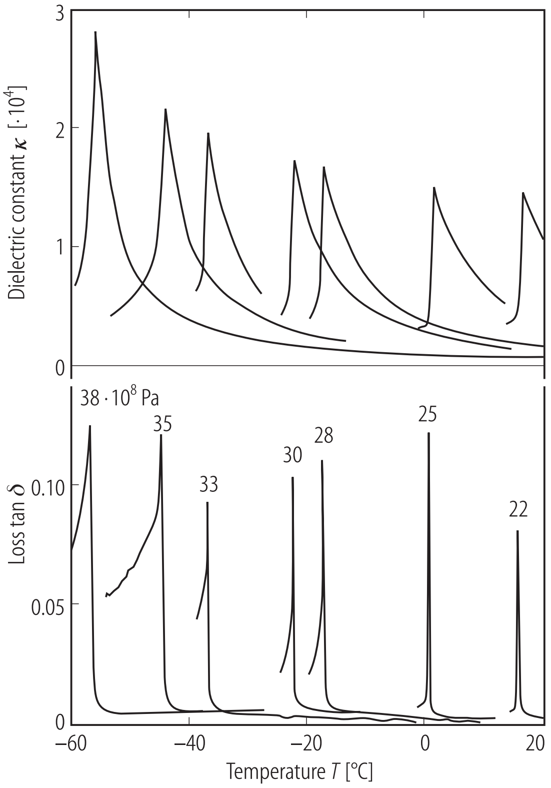

Fig. 1A-10-032. $BaTiO_3$. κ, $\tan\delta$ vs. T [89Dec]. Parameter: p. f = 10 kHz.

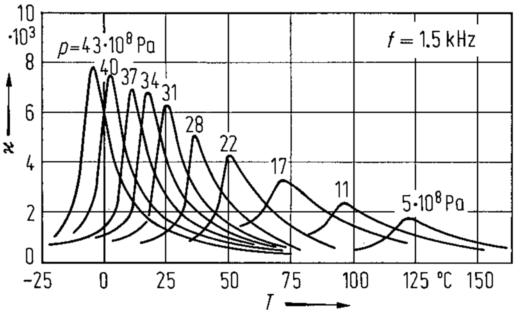

Fig. 1A-10-033. BaTiO$_3$. κ vs. T [77Cla]. Parameter: p. f = 1.5 kHz.

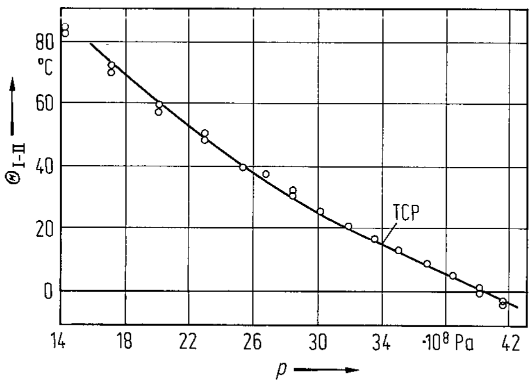

Fig. 1A-10-034. $BaTiO_3$. Θ_{II-I} vs. *p* [77Cla]. TCP: tricritical point.

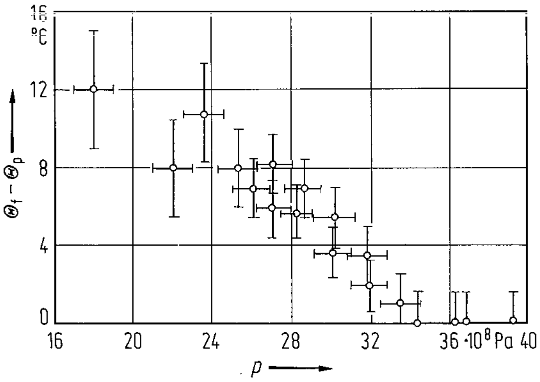

Fig. 1A-10-035. $BaTiO_3$. $\Theta_f - \Theta_p$ vs. p [77Cla]. Θ_f: ferroelectric transition temperature. Θ_p: paraelectric Curie temperature in the Curie-Weiss law.

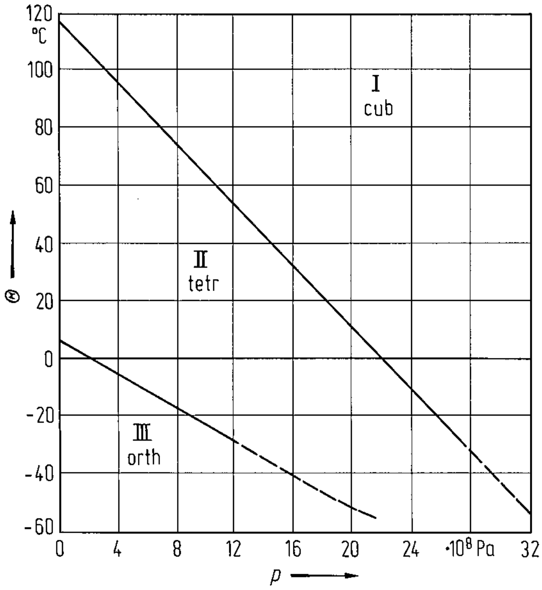

Fig. 1A-10-036. $BaTiO_3$. Θ vs. p [66Sam].

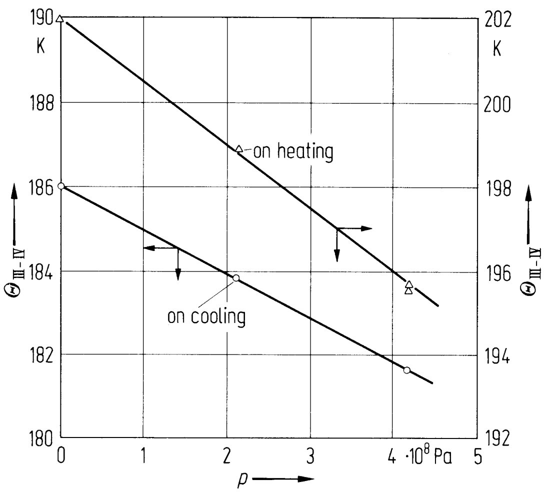

Fig. 1A-10-037. $BaTiO_3$. Θ_{III-IV} vs. p [71Sam].

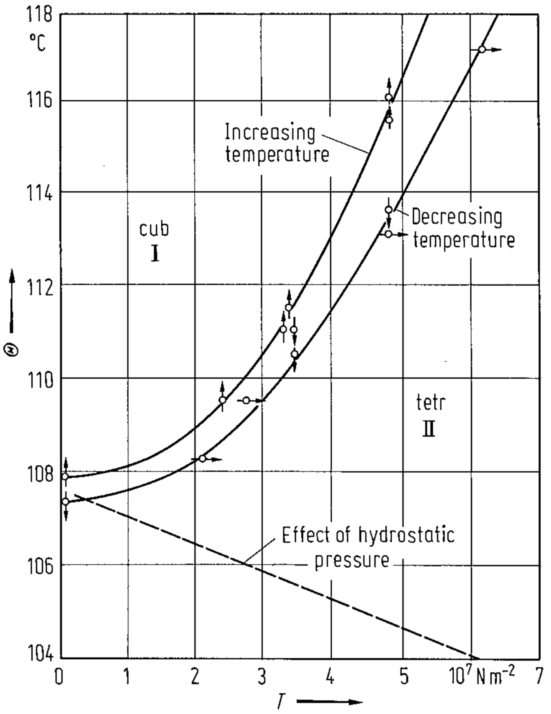

Fig. 1A-10-038. $BaTiO_3$. *Θ* vs. *T* [54For]. *T*: two-dimensional pressure perpendicular to [001].

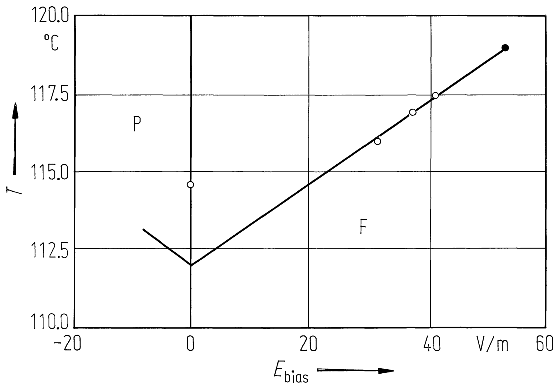

Fig. 1A-10-039. $BaTiO_3$. Phase diagram [85McW]. The line of the first order phase transition terminates at the critical point (full circle).

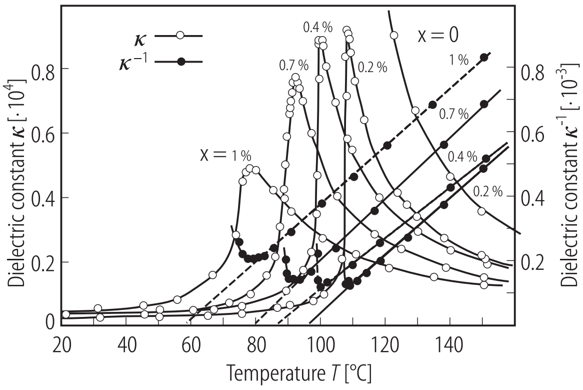

Fig. 1A-10-040. $BaTiO_3$: Co. κ, κ^{-1} vs. T [81God]. Parameter: x. x: Co concentration [%]. $2\pi f = 10^4$ rad s^{-1}.

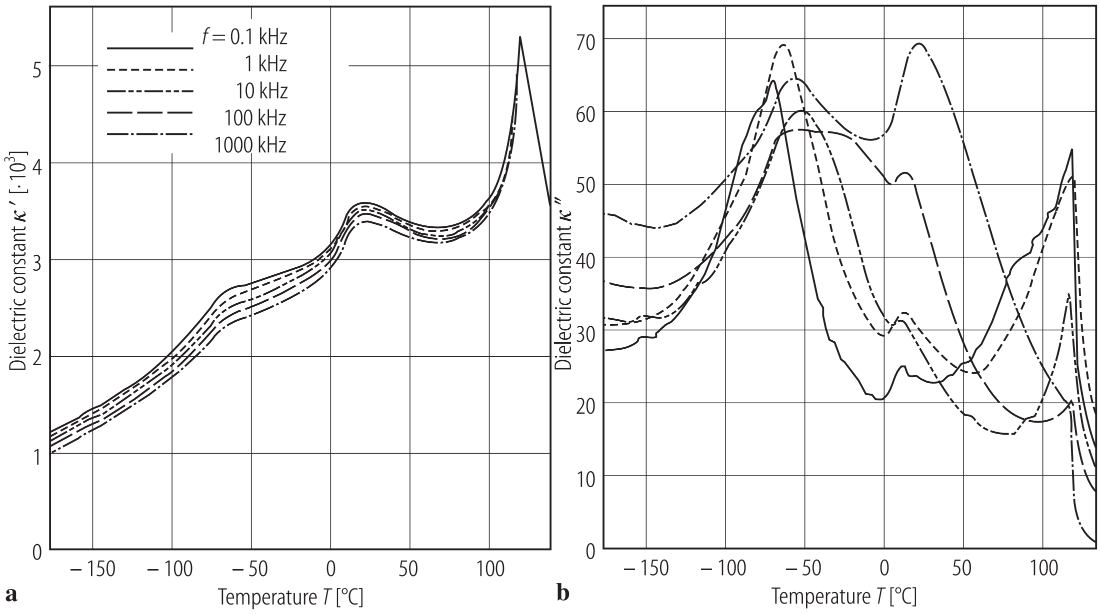

Fig. 1A-10-041. $BaTiO_3$ (ceramics). κ' , κ'' vs. *T* [89Hal]. Parameter: *f*. Grain size: ≈0.5 µm.

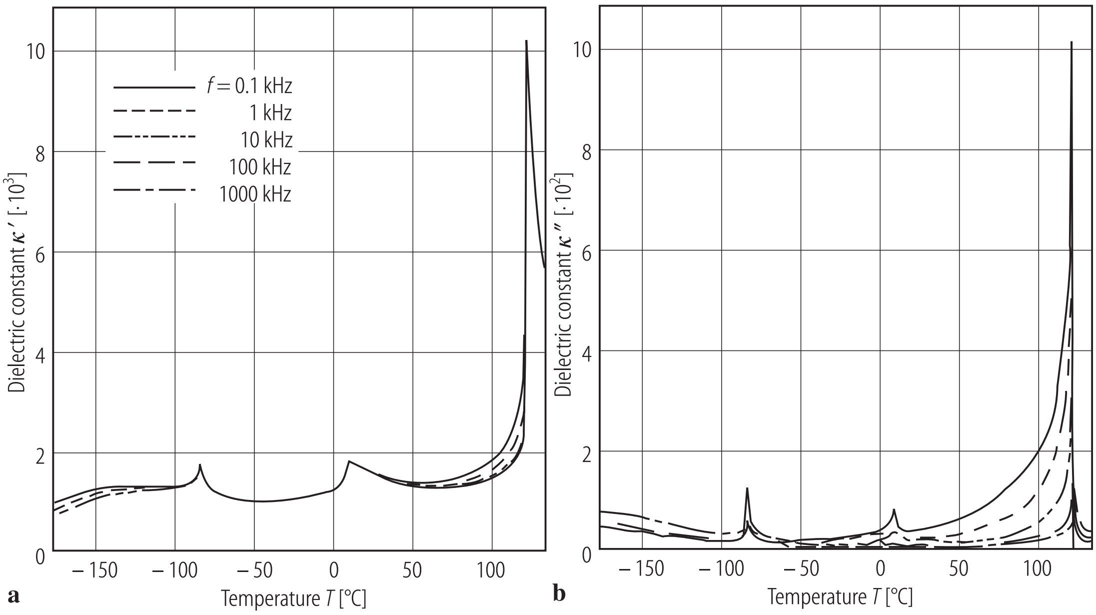

Fig. 1A-10-042. $BaTiO_3$ (ceramics). *κ*' , *κ*'' vs. *T* [89Hal]. Parameter: *f*. Grain size: 10...50 µm.

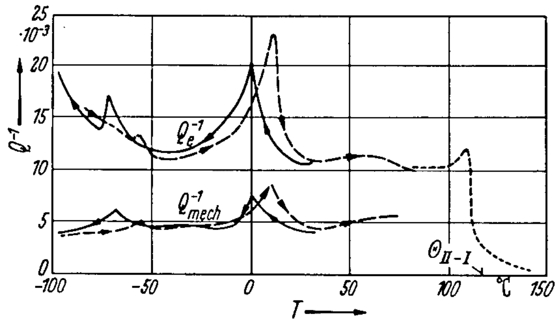

Fig. 1A-10-043. BaTiO$_3$ (ceramics). Q_e^{-1}, Q_{mech}^{-1} vs. T [58Ike]. $Q_e^{-1} = \tan\delta$.

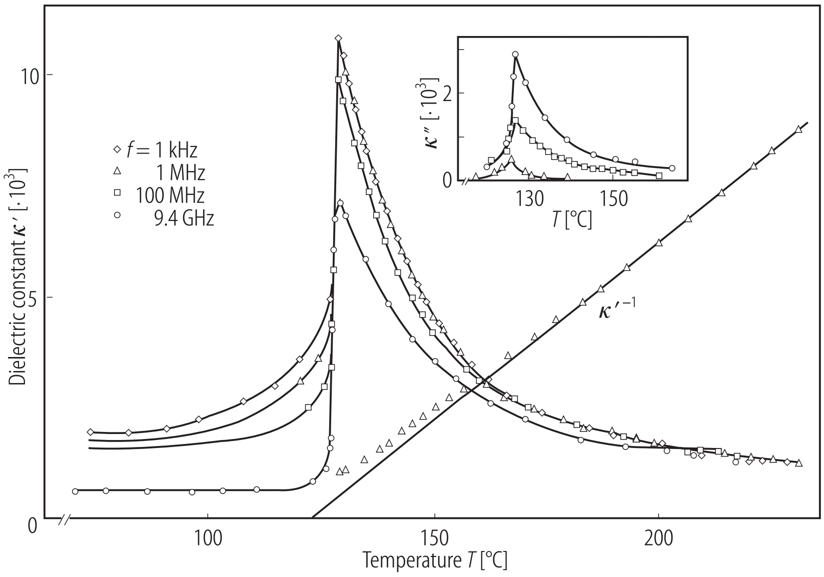

Fig. 1A-10-044. $BaTiO_3$ (ceramics). *κ*' , *κ*'$^{-1}$, *κ*" vs. *T* [88Ker]. Parameter: *f*. Average grain size: 30 µm.

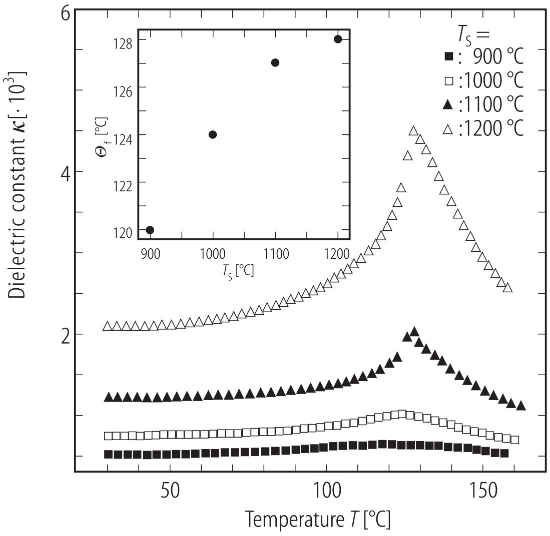

Fig. 1A-10-045. $BaTiO_3$ (ceramics). κ vs. T [94Yas]. Parameter: T_s. T_s: sintering temperature. f = 100 kHz. Insert: Θ_f vs. T_s.

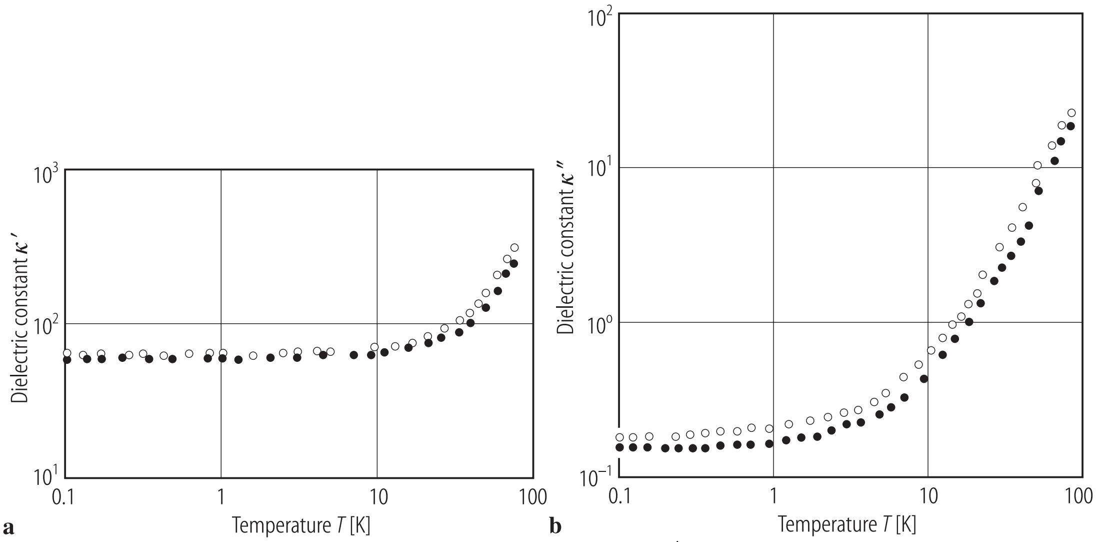

Fig. 1A-10-046. $BaTiO_3$ (ceramics). κ', κ'' vs. *T* [86Zim]. $f = 10^4$ Hz. Open circles: unpolarized. Full circles: polarized.

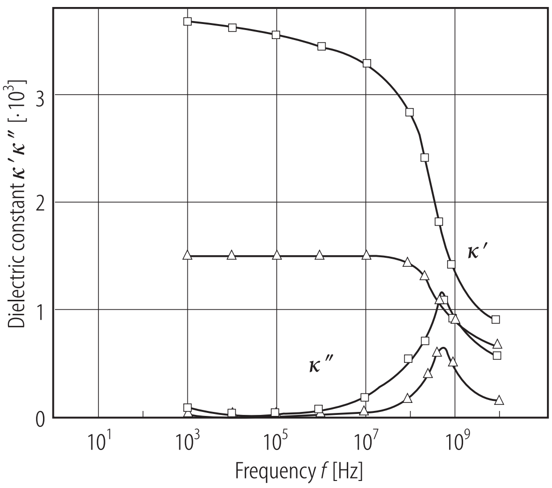

Fig. 1A-10-047. BaTiO$_3$ (ceramics). κ', κ'' vs. f [88Ker]. Squares: grain size < 5 µm. Triangles: grain size > 30 µm. T = RT.

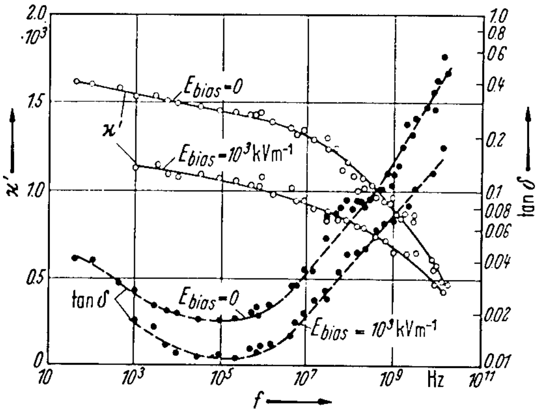

Fig. 1A-10-048. $BaTiO_3$ (ceramics). κ', $\tan\delta$ vs. f [64Pop]. Parameter: E_{bias}.

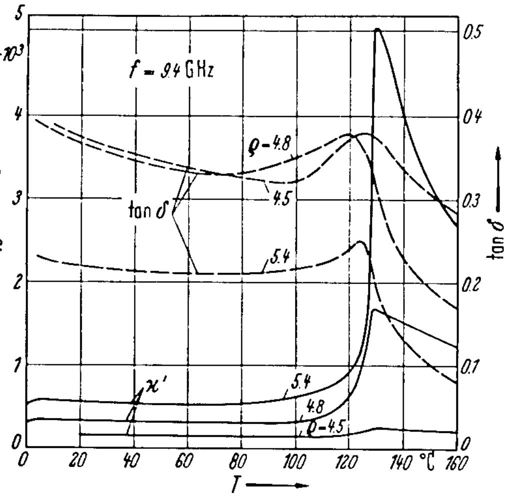

Fig. 1A-10-049. $BaTiO_3$ (ceramics). κ', $\tan\delta$ vs. T at 9.4 GHz [57Sch]. Parameter: p. ρ: density in $10^3\ \mathrm{kg\,m^{-3}}$.

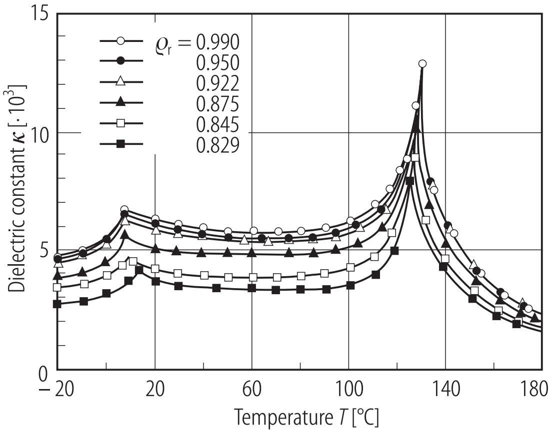

Fig. 1A-10-050. $BaTiO_3$ (ceramics). κ vs. T [93Fan]. Parameter: ρ_r, relative density. f =1 kHz.

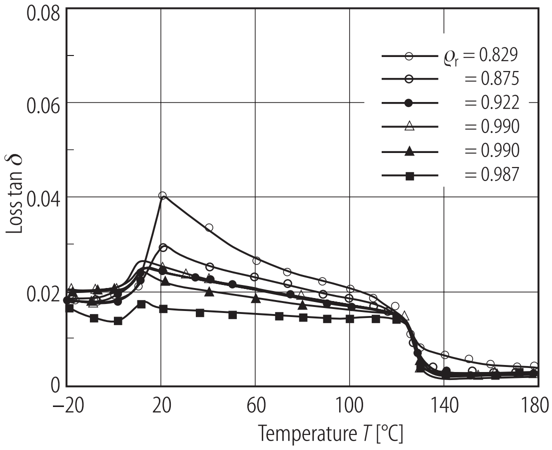

Fig. 1A-10-051. $BaTiO_3$ (ceramics). $\tan\delta$ vs. T [93Fan]. Parameter: ρ_r, relative density. f =1 kHz.

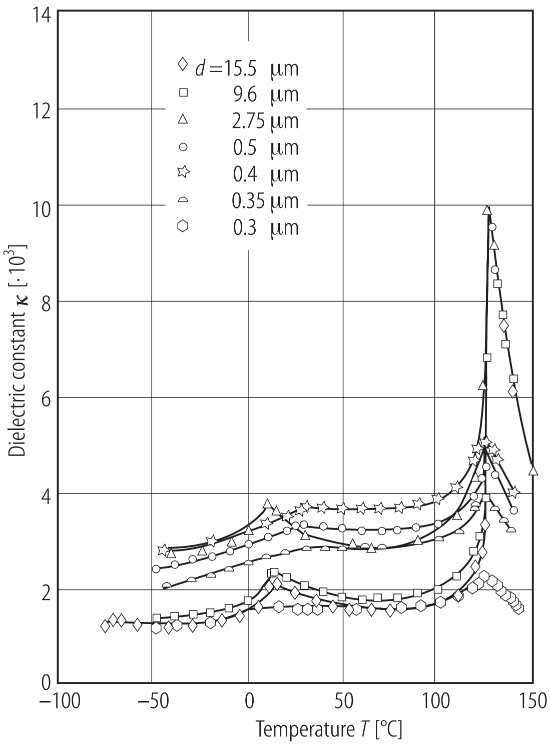

Fig. 1A-10-052. $BaTiO_3$ (ceramics). κ vs. T [89Sha]. Parameter: d, average grain size. f =1 kHz.

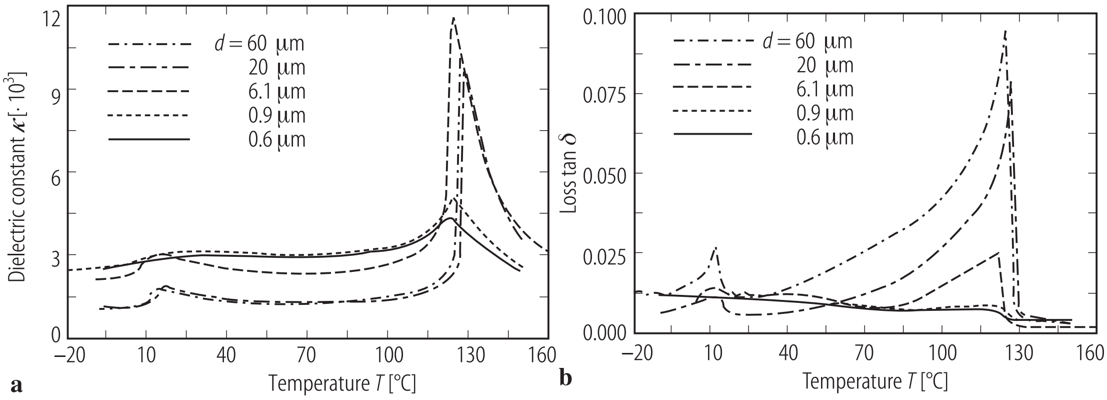

Fig. 1A-10-053. $BaTiO_3$ (ceramics). κ (**a**), tan δ (**b**) vs. T [92WuK2]. Parameter: d, average grain size.

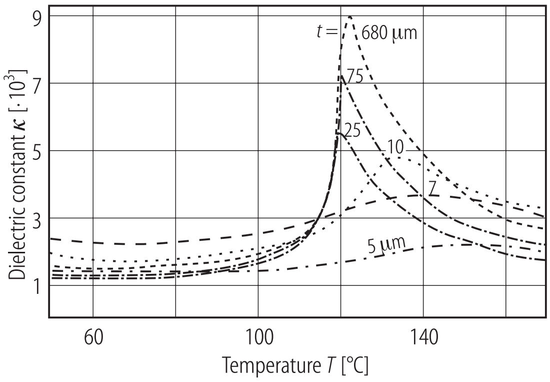

Fig. 1A-10-054. $BaTiO_3$ (ceramics). κ vs. T [81Dam]. Parameter: t, thickness of the specimens. f = 1.56 kHz.

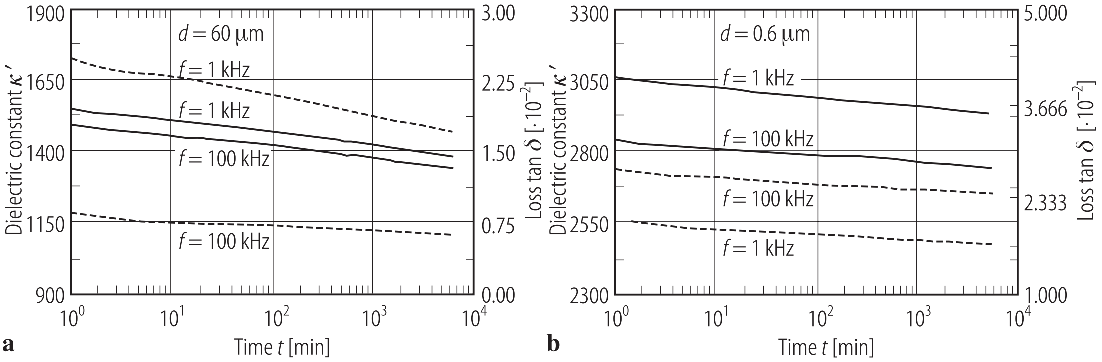

Fig. 1A-10-055. $BaTiO_3$ (ceramics). κ' (**a**), $\tan\delta$ (**b**) vs. t [92WuK2]. Parameter: f. t: aging time at 25 °C. Full lines: κ'. Dotted lines: $\tan\delta$. (**a**): d = 60 µm. (**b**): d = 0.6 µm. d: average grain size.

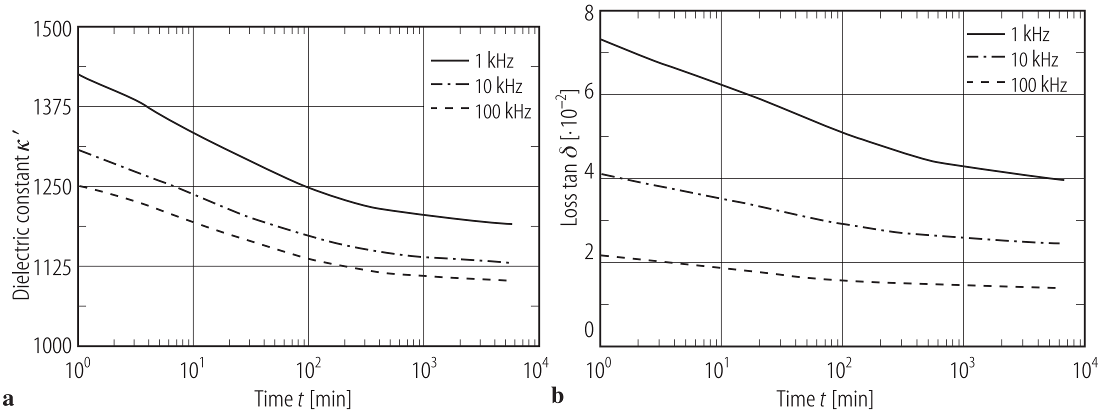

Fig. 1A-10-056. $BaTiO_3$ (ceramics). κ' (**a**), $\tan\delta$ (**b**) vs. t [92WuK2]. Parameter: f. t: aging time at 80 °C. The average grain size d = 60 µm.

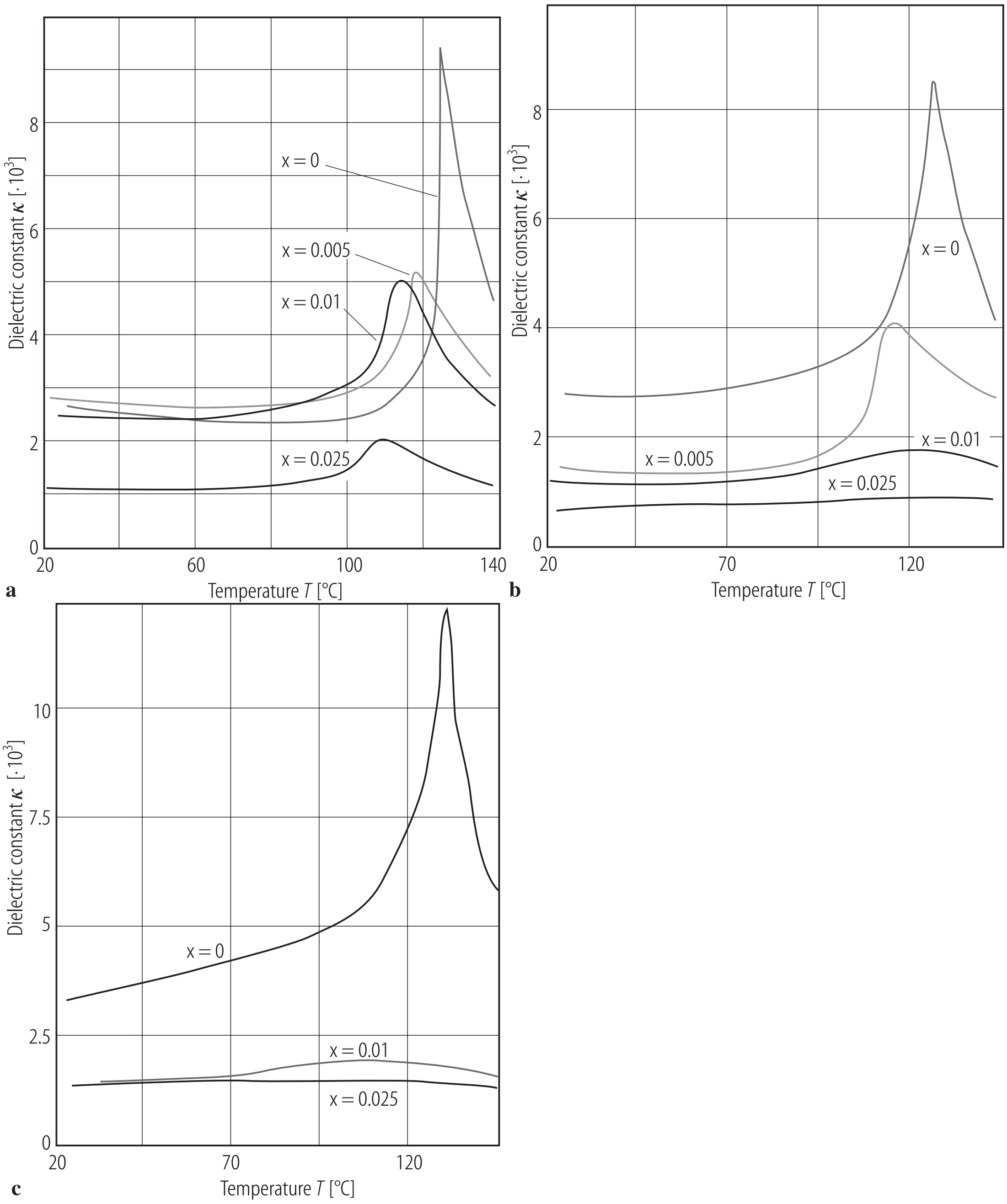

Fig. 1A-10-057. $BaTi_{1-x}Mn_xO_3$ (ceramics). κ vs. T for specimens sintered under different oxygen pressure p_O [90Bat]. Parameter: x. **(a)** $p_O = 2 \cdot 10^4$ Pa. **(b)** $p_O = 10^{-2}$ Pa. **(c)** $p_O = 10^{-6}$ Pa. $f = 1$ kHz.

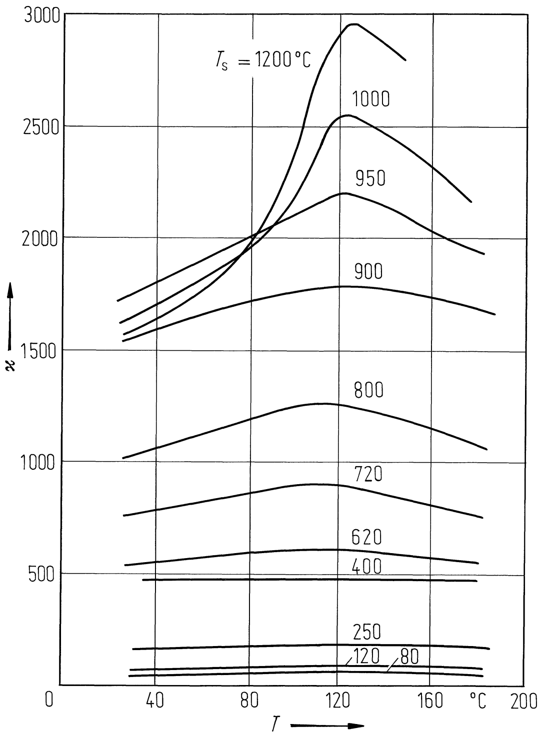

Fig. 1A-10-058. $BaTiO_3$ (thin film). κ vs. T [81Dud1]. Parameter: T_s, temperature of substrate for deposition.

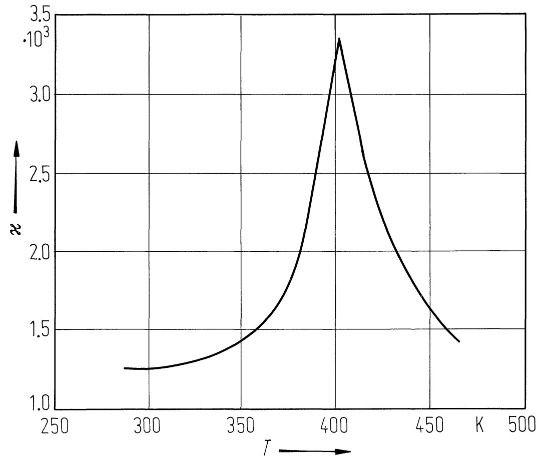

Fig. 1A-10-059. $BaTiO_3$ (thin film). κ vs. T [84Bir].